Imaging Angiogenesis Using ^{99m}Tc-Macroaggregated Albumin Scintigraphy in Patients with Peripheral Artery Disease

Gen Takagi[1], Masaaki Miyamoto[1], Yoshimitsu Fukushima[2], Masahiro Yasutake[1], Shuhei Tara[1], Ikuyo Takagi[1], Naoki Seki[3], Shinichiro Kumita[2], and Wataru Shimizu[1]

[1]Department of Cardiovascular Medicine, Nippon Medical School, Tokyo, Japan; [2]Department of Radiology, Nippon Medical School, Tokyo, Japan; and [3]FUJIFILM RI Pharma Co., Ltd., Tokyo, Japan

One problem of vascular angiogenesis therapy is the lack of reliable methods for evaluating blood flow in the microcirculation. We aimed to assess whether ^{99m}Tc-macroaggregated albumin perfusion scintigraphy (^{99m}Tc-MAA) predicts quantitated blood flow after therapeutic angiogenesis in patients with peripheral artery disease. **Methods:** Forty-six patients with peripheral artery disease were treated with bone marrow mononuclear cell implantation (BMCI). Before and 4 wk after BMCI, blood flow was evaluated via transcutaneous oxygen tension ($TcPO_2$), ankle-brachial index, intravenous ^{99m}Tc-tetrofosmin perfusion scintigraphy (^{99m}Tc-TF), and intraaortic ^{99m}Tc-MAA. **Results:** Four weeks after BMCI, $TcPO_2$ improved significantly (20.4 ± 14.4 to 36.0 ± 20.0 mm Hg, $P < 0.01$), but ankle-brachial index did not (0.65 ± 0.30 to 0.76 ± 0.24, $P = 0.07$). Improvement in ^{99m}Tc-TF count (0.60 ± 0.23 to 0.77 ± 0.29 count ratio/pixel, $P < 0.01$) and ^{99m}Tc-MAA count (5.21 ± 3.56 to 10.33 ± 7.18 count ratio/pixel, $P = 0.02$) was observed in the foot region but not the lower limb region, using both methods. When these data were normalized by subtracting the pixel count of the untreated side, the improvements in ^{99m}Tc-TF count (−0.04 ± 0.26 to 0.08 ± 0.32 count ratio/pixel, $P = 0.04$) and ^{99m}Tc-MAA count (1.49 ± 3.64 to 5.59 ± 4.84 count ratio/pixel, $P = 0.03$) in the foot remained significant. ^{99m}Tc-MAA indicated that the newly developed arteries were approximately 25 μm in diameter. **Conclusion:** BMCI induced angiogenesis in the foot, which was detected using ^{99m}Tc-TF and ^{99m}Tc-MAA. ^{99m}Tc-MAA is a useful method to quantitate blood flow, estimate vascular size, and evaluate flow distribution after therapeutic angiogenesis.

Key Words: angiogenesis; bone marrow mononuclear cells; peripheral artery disease; radionuclide imaging; sensitivity and specificity

J Nucl Med 2016; 57:192–197
DOI: 10.2967/jnumed.115.160937

Peripheral artery disease, which is mainly due to atherosclerosis, has a poor prognosis (*1*) and is increasingly becoming a worldwide problem (*2*). Recently, the therapeutic focus has shifted to regenerative techniques that induce angiogenesis. Human bone marrow is a diverse reservoir for several progenitor cell populations, including endothelial progenitor cells (EPCs) (*3*). The use of progenitor cells (stem cells) for cell-based regenerative therapy is promising because of the high proliferative capacity and multilineage differentiation potential of the progenitor cells and also because of their contribution to angiogenesis or arteriogenesis (*4*) through the recruitment of EPCs (*5*) and their functionality and secretion of growth factors (*6*) and cytokines (*7–9*) that promote cell survival. Thus, many approaches to therapeutic angiogenesis have been investigated (*10–13*). We have investigated therapeutic angiogenesis using bone marrow mononuclear cell implantation (BMCI) and have accumulated clinical evidence for different populations (*12,14,15*). To resolve the issue of the lack of a reliable technique for blood flow analysis at the microcirculation level, one of the aims of this study was to establish a method for analysis of angiogenesis by quantitative radionuclide determination to evaluate blood flow in terms of the target-to-background ratio (TBR), which references the brain count as a control, as we previously reported (*12,14,15*). A secondary aim was to confirm the location of improved blood flow using the radioisotope examination. Previous reports have evaluated the localization of perfusion using ^{99m}Tc-macroaggregated albumin (^{99m}Tc-MAA) (*16–18*). However, the results are difficult to interpret. A third aim of this study was to estimate the sizes of new arteries that are smaller than visible arteries (<200 μm). In this context, we hypothesized that radionuclide assessment after BMCI would be advantageous. ^{99m}Tc-MAA has been used almost universally as the perfusion agent for lung scintigraphy. After intravascular injection of ^{99m}Tc-MAA, radioisotope particles are lodged in the capillaries and precapillary arterioles of the target vessels in proportion to perfusion (*19*), and this is less affected by inflammation. ^{99m}Tc-MAA perfusion scintigraphy is a suitable method to confirm the presence of angiogenesis-related microvascular blood flow. In this investigation, we performed a quantitative analysis of perfusion, determined blood flow distribution, and estimated vessel size after BMCI using ^{99m}Tc-MAA perfusion scintigraphy as well as estimated the diagnostic accuracy.

MATERIALS AND METHODS

Study Design and Participants

We enrolled 46 consecutive patients (mean age ± SD, 59.8 ± 13.7 y; 63% men) with arteriosclerosis obliterans or thromboangiitis obliterans from September 2011 to December 2012 who had rest pain or ischemic ulcer (Fontaine class 3 to 4, Rutherford class III-4 to III-6) for more than 3 mo under standard treatment but were not eligible for bypass surgery or endovascular catheter treatment. Exclusion criteria were active infection confirmed by blood examination or the presence of osteomyelitis; no evidence of angiologic stenosis; vascular surgery within the previous 30 d; active malignancy as determined by endoscopy, tumor marker, or fecal occult blood testing or history of cancer treatment within the past 5 y; untreated proliferative diabetic retinopathy; current smoker; addiction

Received May 22, 2015; revision accepted Oct. 19, 2015.
For correspondence or reprints contact: Gen Takagi, Department of Cardiovascular Medicine, Nippon Medical School, 1-1-5 Sendagi, Bunkyo-ku, Tokyo 113-8603, Japan.
E-mail: gen52@nms.ac.jp
Published online Nov. 5, 2015.

to alcohol or any other drug; evidence of viral infection (HBV, HCV, HIV); complications of any serious disease affecting the patient's general condition, such as organic brain disease or heart, lung, kidney, or liver failure; and inability to participate in radionuclide imaging studies before and after the BMCI. This study was performed at the Nippon Medical School Hospital and was approved by the Institutional Review Board (ethical committee of Nippon Medical School), and all patients provided written informed consent. The protocol was registered with the University Hospital Medical Information Network-Clinical Trial Registry (UMIN-CTR), which is accepted by the International Committee of Medical Journal Editors (no. UMIN000006166).

BMCI

Bone marrow mononuclear cells were injected in the calf and foot muscles of the ischemic limbs as previously described in detail (*14,15*). Briefly, bone marrow (400–600 mL) was collected from the bilateral iliac bones under general anesthesia. The mononuclear cell fraction was sorted, and 60–100 mL of the cell suspension were processed by a cell separator (AS-TEC 204; Fresenius Kabi). As bone marrow aspirates were being processed, necrotic tissue was surgically debrided under sterile conditions. Thereafter, the cell suspension (1 mL/point) was injected intramuscularly. Cell injection was performed using guidance from a marked transparent overlay, which helped to ensure that cells were evenly injected, at 1 mL per site, into the entire ischemic area of the below-knee muscles. Finally, skin grafting was performed to cover the ulcers unless there was spontaneous epithelialization of the wound margin.

Flow cytometry was performed with the bone marrow cells for quality analysis of the mononuclear cell count, including EPCs, as described previously (*20*). Briefly, EPCs were analyzed for the expression of CD34, CD45, CD133, and vascular endothelial growth factor receptor-2 (VEGFR-2) using 4-color flow cytometry (FACSCalibur; BD Biosciences). Samples were incubated with anti-CD34 FITC (Beckman Coulter Inc.), anti-CD45-PerCP (BD Biosciences), anti-CD133/2 (293C3)-APC (Miltenyi Biotec GmbH), and phycoerythrin-conjugated anti–VEGFR-2 (R&D Systems, Inc.) for 40 min at 4°C, followed by erythrolysis via the addition of a lysing reagent, and then washed once with 0.2% phosphate-buffered saline with bovine serum albumin. CD34+ cells were analyzed using sequential gating strategies. A CD45 versus side scatter dot plot was set to include all CD45+ events, and CD45+ events were set to include all nucleated white blood cells and to exclude red blood cells, nucleated red blood cells, platelets, and other cellular debris, which do not express CD45. CD45+ cells were gated on a forward-scatter versus side-scatter dot plot to confirm the mononuclear cell fraction. Mononuclear cells formed a cluster with low side-scatter and low to intermediate forward-scatter. CD34+ and CD45dim cells in the mononuclear cell fraction were gated on a forward-scatter versus side-scatter dot plot to obtain a cluster of true CD45dim CD34+ cells. True CD45dim and CD34+ events were displayed on a CD133 versus VEGFR-2 dot plot, and then the resulting population was examined for the dual expression of VEGFR-2 and CD133. CD45dim/CD34+/CD133+/VEGFR-2+ cells were enumerated in the upper right quadrant of the plot. At least 2,000,000 events were measured in the CD45+ gate. Data were analyzed using CELLQuest (BD Biosciences). The EPC values were defined as the percentage of CD34+, CD45dim, CD133+, and VEGFR-2+ cells per CD34+CD45dim cell fraction.

Clinical Assessment

The visual analog pain scale (mm) and maximum walking distance were evaluated. The visual analog pain scale scored maximal pain as 100 and minimal pain as 0. The maximum walking distance was determined using a standard treadmill test. Specialized personnel supervised the exercise tests. All patients were asked to walk on a treadmill at a speed of 3.1 km/h for a maximum of 5 min. No inclining-plane protocol was used. Patients were encouraged to finish the whole test, but it was stopped when the patient was unable to walk further. The time and walking distance until the occurrence of leg pain and the total walking time and distance were recorded.

Several parameters were evaluated to quantify recovery of local blood flow. The ankle-brachial index (ABI) (Omron Healthcare Co. Ltd.) was measured using standard methods and calculated as the ratio of ankle to brachial pressure. Tissue oxygen content was measured as transcutaneous oxygen tension ($TcPO_2$) with a TCM 400 monitor (Radiometer, Inc.). The transducer was placed on the dorsum of the ischemic limb and warmed to 43.5°C to increase skin permeability to oxygen molecules at the measurement site. Consistent $TcPO_2$ data were collected for approximately 20 min with the patient resting supine and breathing room air.

^{99m}Tc-TF radionuclide imaging was performed on 46 patients using a previously reported method (*14,15*). ^{99m}Tc-TF (740 MBq; total volume, 1.25 mL) was injected intravenously. The ^{99m}Tc-TF data were used to enable comparison and examination of ^{99m}Tc-MAA scintigraphy. ^{99m}Tc-MAA imaging analysis was performed for 11 patients who successfully underwent angiography. All other patients who did not undergo angiography were excluded from the ^{99m}Tc-MAA study. ^{99m}Tc-MAA scintigraphy was performed as follows: a pig-tail catheter was placed in the descending aorta below the renal artery and just above the iliac bifurcation, and 296 MBq of commercial ^{99m}Tc-MAA (Nihon Medi-Physics Co., Ltd.) were injected into the artery in an antegrade fashion. The ^{99m}Tc-MAA consisted of 1.7 mg of human serum macroaggregated albumin (24×10^4 particles; total volume, 19.8 mL) in which 95% of the ^{99m}Tc was bound to the MAA.

Data were acquired in a 256 × 1,024 matrix on the 140-keV photopeak of ^{99m}Tc. Approximately 12 min after injection of the radiotracer, whole-body scintigraphy was performed with the patient prone in both anterior and posterior projections with a dual-head large-field-of-view γ-camera (ADAC Vertex; Philips). Each head of the γ-camera was equipped with a low-energy, high-resolution collimator. The scan speed was 120 mm/min, and the image acquisition time was approximately 15 min. The data were averaged for quantitative analysis. To analyze the data acquired from ^{99m}Tc-TF and ^{99m}Tc-MAA scintigraphy, regions of interest of equal surface area were drawn around the appropriate muscle group (calf muscles and foot) in the anterior and posterior projections. After the radionuclide count within the regions of interest was determined, intracranial (brain) uptake was calculated as the background. The TBR was defined as the average counts per pixel in each muscle/the average counts per pixel in the brain. Examinations were performed before and at 4 wk after therapy. To avoid bias, the actual change in blood flow was analyzed by subtracting the pixel count of the untreated limb from that of the treated limb. Granulometric analysis of ^{99m}Tc-MAA microparticles was performed by a laser diffraction particle size analyzer (Sald-7000; Shimadzu Scientific Instruments), and the diameter was visually confirmed under a microscope after staining with a 1% 4,5,6,7-tetrachloro-2′,4′,5′,7′-tetraiodofluorescein solution. Samples from 3 lots were analyzed to determine these measurements and averaged. Granulometric analysis was performed by FujiFilm RI Pharma Co., Ltd. All data were collected retrospectively.

Patients were monitored for major adverse cardiovascular events until 4 wk after BMCI. Major adverse cardiovascular events were defined as all-cause mortality, nonfatal myocardial infarction (including silent myocardial infarction), stroke, acute coronary syndrome, and endovascular or surgical intervention on the coronary or leg arteries. In addition, patients were followed for 1 y to monitor for amputation-free limb survival and major adverse events.

Statistical Analysis

Exact 2-sided 95% confidence intervals (CIs) were evaluated using a binominal distribution. The association between BMCI and the untreated side was examined using 2-way repeated-measures ANOVA.

TABLE 1
Patient Characteristics

Characteristic	Mean ± SD or *n*
Age (y)	59.8 ± 13.7
Sex	
Male	29 (63.0)
Female	17 (37.0)
Diagnosis	
Arteriosclerosis obliterans	34 (53.9)
Thromboangiitis obliterans	12 (26.1)
Ischemic status	
Fontaine 3	10 (21.7)
Fontaine 4	36 (78.3)
Smoking history	26 (56.5)
Complications	
Diabetes mellitus	23 (50.0)
Hypertension	27 (58.7)
Dyslipidemia	24 (47.8)
Chronic kidney disease on hemodialysis	9 (19.6)
Bone marrow cells (in total)	$4.8 \pm 3.7 \times 10^9$ (95% CI, $3.4–6.2 \times 10^9$)
CD34+ cells	490.9 ± 368 cells/μL

Data in parentheses are percentage of patients unless otherwise indicated.

Within-treatment analyses of changes were performed using a Wilcoxon rank-sum test. Cohen's κ coefficient analysis was used to test for better-than-chance agreement between 2 observers (radiologists). For intraobserver comparisons, at least 2 examinations from each patient were assessed by each observer, and the observers were masked to the patient's clinical condition.

Considering the high rate of limb amputations in the nontreatment group, untreated limbs in treated patients were used as controls. The sensitivity and specificity of radioisotope detection were calculated with $TcPO_2$ threshold against limb amputation as the standard and used to determine likelihood ratios. For a positive change in the TBR, the likelihood ratio was calculated as sensitivity/1 – specificity; for a negative change in the TBR, the likelihood ratio equaled 1 – sensitivity/specificity. A 95% CI was calculated for every measure. The amputation-free limb survival rate and the occurrence of major adverse events within the 1-y follow-up period were assessed using a χ^2 analysis. A P value of less than 0.05 was considered statistically significant. All statistical analyses were performed using SPSS statistics software (version 20; IBM Corp.).

RESULTS

The baseline characteristics of the study participants are shown in Table 1. Improvements were seen in the indicators of clinical effectiveness. The visual analog pain scale decreased significantly, from 79.7 ± 23.8 at baseline to 9.2 ± 12.0 at 4 wk after BMCI ($P < 0.01$), and maximum walking distance increased significantly, from 94.3 ± 78.5 to 258.0 ± 141.1 m ($P < 0.01$) (Fig. 1). Skin perfusion increased significantly 4 wk after BMCI, as indicated by a change in $TcPO_2$ from 20.4 ± 14.4 at baseline to 36.0 ± 19.8 mm Hg at 4 wk ($P < 0.01$), whereas the ABI did not change significantly (0.65 ± 0.30 to 0.76 ± 0.24, $P = 0.07$) (Fig. 2). ABI in the

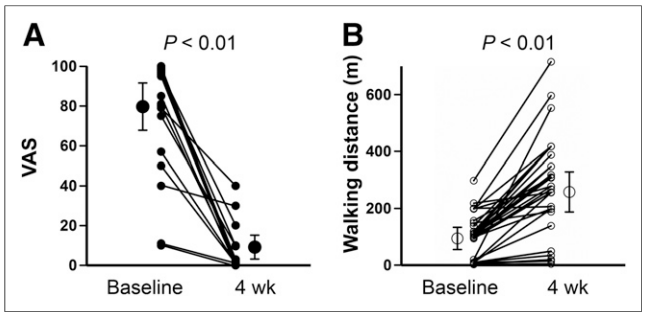

FIGURE 1. Visual analog scale (VAS) and maximum walking distance. Graphs show significant improvement in VAS score (A) and maximum walking distance (B) at 4 wk after therapy.

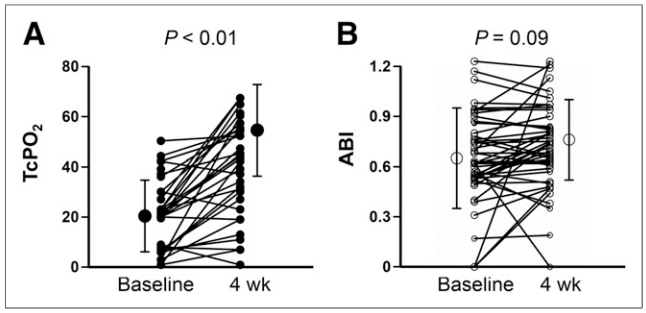

FIGURE 2. $TcPO_2$ and ABI. $TcPO_2$ (A) was significantly improved 4 wk after therapy. However, there was no significant change in ABI (B).

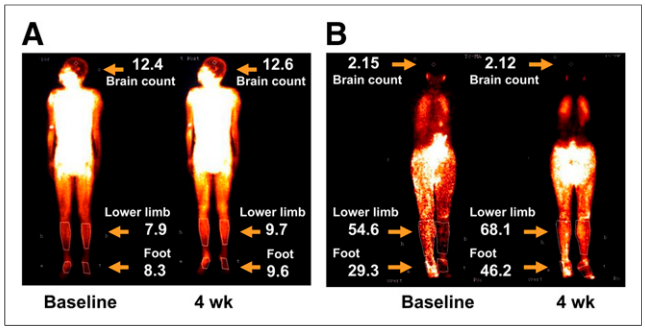

FIGURE 3. Representative radioisotope images of angiogenesis using ^{99m}Tc-TF and ^{99m}Tc-MAA perfusion scintigraphy. (A) Representative ^{99m}Tc-TF study from patient who underwent BMCI in ischemic left leg. (B) Representative ^{99m}Tc-MAA study in patient who underwent BMCI in ischemic right leg.

nontreated leg indicated no significant changes (0.86 ± 0.28 to 0.89 ± 0.27, $P = 0.65$).

In the assessment of angiogenesis by radionuclide imaging (representative images are shown in Fig. 3), significant increase in the ^{99m}Tc-TF score was seen in the foot region in both the treated limb (0.60 ± 0.23 to 0.77 ± 0.29 count ratio/pixel, $P < 0.01$, Fig. 4A) and the untreated limb (0.64 ± 0.20 to 0.70 ± 0.24 count ratio/pixel, $P = 0.04$, Fig. 4A). The scores were changed significantly in the lower leg region at 4 wk after BMCI (treated limb, 1.03 ± 0.27 to 1.18 ± 0.38, $P < 0.01$; untreated limb, 1.01 ± 0.28 to 1.16 ± 0.34, $P < 0.01$, Fig. 4B). On the other hand, the ^{99m}Tc-MAA score was improved significantly in the foot region of the treated limb at 4 wk after treatment (5.21 ± 3.56 to 10.33 ± 7.18 count ratio/pixel, $P = 0.02$, Fig. 4C), compared with the untreated side (3.82 ± 1.63 to 6.05 ± 6.07, $P = 0.33$, Fig. 4C), but not in the lower leg region (treated limb, 5.28 ± 3.63 to 11.79 ± 10.22, $P = 0.09$; untreated limb, 6.17 ± 4.40 to 10.85 ± 8.90, $P = 0.09$, Fig. 4D).

The interaction between the BMCI-treated side and the untreated side were compared (Fig. 4). There were significant interactions in the TBR in the foot region for both ^{99m}Tc-TF ($P = 0.01$, 2-way repeated-measures ANOVA between the 2 regions, Fig. 4A) and ^{99m}Tc-MAA ($P = 0.01$, 2-way repeated-measures ANOVA between the 2 regions, Fig. 4C). However, no interaction was observed in the lower leg region for ^{99m}Tc-TF ($P = 0.94$, 2-way repeated-measures ANOVA between the 2 limbs, Fig. 4B) or ^{99m}Tc-MAA ($P = 0.31$, 2-way repeated-measures ANOVA between the 2 regions, Fig. 4D). The net gain in blood flow (Fig. 5) was calculated by subtracting the pixel count of the untreated limb from that of the treated limb and is expressed as a normalized score. The normalized ^{99m}Tc-TF score in the foot region improved significantly after BMCI (−0.04 ± 0.26 to 0.08 ± 0.32, $P = 0.04$, Fig. 5A), but no improvement was observed in the lower leg region (0.01 ± 0.20 to 0.01 ± 0.26, $P = 0.97$, Fig. 5B). In addition, the normalized ^{99m}Tc-MAA score in the foot region improved significantly (1.49 ± 3.64 to 5.59 ± 4.84, $P = 0.04$, Fig. 5C), but no significant changes were observed in the lower leg region (−0.17 ± 4.36 to 1.55 ± 5.14, $P = 0.45$, Fig. 5D). There was no difference in TBR associated with disease type.

Regarding the reliability of the TBR assessment, the linear-weighted κ values indicated a moderate interobserver agreement of 0.710 and intraobserver agreement of 0.667 for ^{99m}Tc-TF, determined after rounding the numeric data to 1 decimal place. Amputation thresholds of $TcPO_2$ and improvement in TBR were assessed at the 4-wk evaluation (χ^2 test; $P = 0.64$ for ^{99m}Tc-TF and $P = 0.024$ for ^{99m}Tc-MAA). The sensitivity, specificity, positive predictive value, negative predictive value, and predictive accuracy for ^{99m}Tc-TF and ^{99m}Tc-MAA are shown in Table 2. The granulometric distribution of ^{99m}Tc-MAA displayed a mean particle size of 25.83 μm, and 92.7% of particles were within 10–60 μm (Fig. 6).

No adverse events occurred during the 4-wk follow-up period. All patients had healed ulcers, and all were able to use the affected foot at discharge. There were 3 major limb amputations and

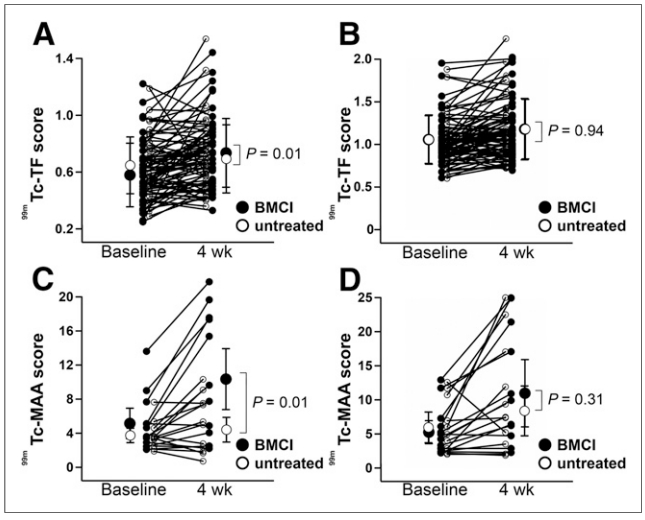

FIGURE 4. Quantitative radionuclide scores from treated and untreated limbs. A and C indicate foot region, and B and D indicate lower leg region. (A and B) ^{99m}Tc-TF perfusion scintigraphy score before and at 4 wk after BMCI. There was significant improvement in foot region of BMCI-treated leg, compared with untreated limb (A), but not in lower leg region (B). (C and D) ^{99m}Tc-MAA perfusion scintigraphy scores before and at 4 wk after BMCI. There was significant improvement in foot region of BMCI-treated leg, compared with untreated limb (C), but not in lower leg region (D).

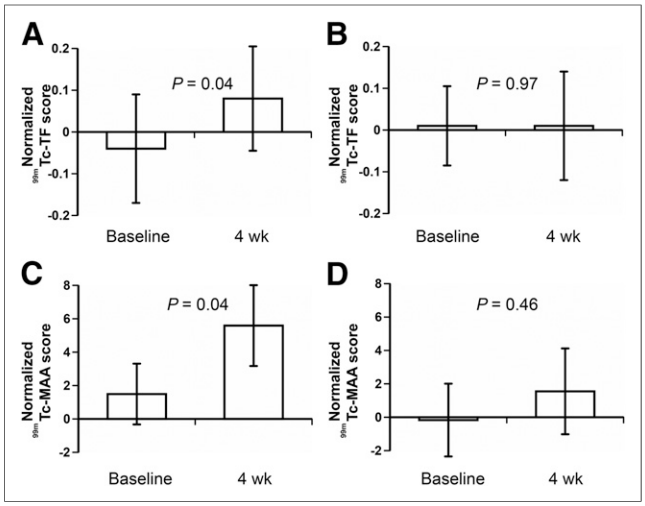

FIGURE 5. Normalized radionuclide scores from treated and untreated limbs. A and C show results from foot region, and B and D show lower leg region. (A and B) ^{99m}Tc-TF perfusion scintigraphy scores before and 4 wk after BMCI. There was significant improvement at 4 wk after BMCI in foot region, compared with untreated limb (A), but not in lower leg region (B). (C and D) ^{99m}Tc-MAA perfusion scintigraphy scores before and at 4 wk after BMCI. There was significant improvement in the foot region after BMCI, compared with untreated limb (C), but not in lower leg region (D).

TABLE 2
Diagnostic Accuracy and Areas Under Receiver-Operator Characteristic Curve

Radionuclide	Sensitivity (%)	Specificity (%)	Positive predictive value (%)	Negative predictive value (%)	AUC
^{99m}Tc-TF	58.3	42.9	77.8	23.1	0.55 (0.30–0.71)
^{99m}Tc-MAA	87.5	100	100	75	0.91 (0.6–1.00)

AUC = area under receiver-operator characteristic curve.
Data in parentheses are 95% confidence intervals.

1 death during the 1-y follow-up period (mean follow-up, 319 d; 95% CI, 291–347). The overall limb salvage rate was 93.5% (mean follow-up, 317 d; 95% CI, 287–348), and the major adverse cardiovascular event-free rate was 93.5% (mean follow-up, 309 d; 95% CI, 274–344). The cutoff value of Δ ^{99m}Tc-TF was 0.11 (determined by receiver-operator characteristic curve), and Kaplan–Meier analysis ($P = 0.005$ by log-rank test) against leg amputation showed significant differences (Supplemental Fig. 1; supplemental materials are available at http://jnm.snmjournals.org). The cutoff for ^{99m}Tc-MAA was not included because no leg amputation was observed in this group.

DISCUSSION

In this study, we identified a reliable means of quantitative analysis of therapeutic angiogenesis after BMCI. To reduce the effect of confounding variables that relate to bilateral limb condition, such as improvements in walking distance and nutritional status (Fig. 1), normalized values were calculated by subtracting the untreated limb count (as an internal control) to confirm the clinical effects of BMCI, and the results showed statistically significant improvement in the foot region on both ^{99m}Tc-TF and ^{99m}Tc-MAA scintigraphy (Fig. 5). We also examined regional recovery after BMCI using specific regions of interest in the lower leg and foot region and successfully showed the regional differences. Furthermore, the scores of both ^{99m}Tc-TF (reference diameter of average triclinic crystal structure size, 1.25 nm) (*21*) and ^{99m}Tc-MAA (reference diameter of average microsphere size, 25 μm) showed improvement at 4 wk after BMCI, providing direct evidence that mature arterial growth was promoted in the ischemic foot area in the 4 wk after BMCI. Blood flow analysis by skin perfusion pressure and $TcPO_2$ have also been useful parameters in several therapeutic angiogenesis protocols (*12,14,15,22,23*). ^{99m}Tc-TF scintigraphy is a useful examination for detection of early phase angiogenesis, as we have reported previously (*14,15*). However, the specificity is lower than that of ^{99m}Tc-MAA, which likely implies that a local inflammatory reaction, such as osteomyelitis or phlebitis (*14,15*), results in a large SD, even in the foot region, when compared with ^{99m}Tc-MAA (Figs. 4A and 5A). Concerning the feasibility of the examination, ^{99m}Tc-TF is useful because it can be performed at the outpatient screening, whereas ^{99m}Tc-MAA requires intraaortic injection. However, ^{99m}Tc-MAA can be performed at the time of diagnostic digital subtraction angiography.

Several limitations of this study deserve mention. Some of the ABI data were indicators of severity of disease. Most of the patients had calcified arteries that made it difficult to obtain correct pressure measurements or to detect ischemia localized only in the foot region. Also, other parameters, such as the skin perfusion pressure or toe pressure, could not be measured because of the location of the ulcers. Nonetheless, tissue ischemia was confirmed by several different modalities, consistent with our previous observations (*15*). The sample size of patients receiving ^{99m}Tc-MAA scintigraphy was small, and data for patients with both arteriosclerosis obliterans and thromboangiitis obliterans were included in the data analysis. Thus, it will be important to confirm these results with a large-scale investigation in a uniformly affected population.

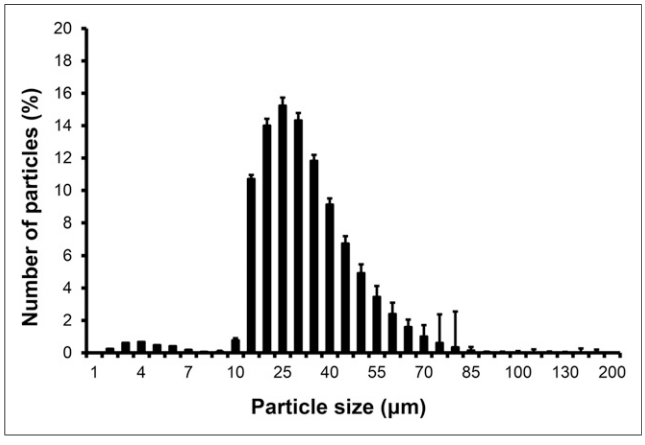

FIGURE 6. Particle size distribution patterns of ^{99m}Tc-MAA microspheres.

CONCLUSION

Radionuclide determination of quantitative score, flow distribution, and vascular size with ^{99m}Tc-MAA appears to be a useful method to evaluate functional blood flow recovery after BMCI. Thus, it may be a reliable approach to confirm therapeutic angiogenesis in the clinical setting. Furthermore, the radionuclide approach is applicable for other angiogenesis protocols such as those using growth factors, genes, or pluripotent stem cells.

DISCLOSURE

The costs of publication of this article were defrayed in part by the payment of page charges. Therefore, and solely to indicate this fact, this article is hereby marked "advertisement" in accordance with 18 USC section 1734. This work was supported by JSPS KAKENHI (Grants-in-Aid for Scientific Research, nos. 20590844 and 24591075) and a Mitsukoshi Health and Welfare Foundation grant. Naoki Seki is an employee of FUJIFILM RI Pharma Co., Ltd. No other potential conflict of interest relevant to this article was reported.

ACKNOWLEDGMENT

We thank Harumi Ohtsubo for technical assistance.

REFERENCES

1. Norgren L, Hiatt WR, Dormandy JA, Nehler MR, Harris KA, Fowkes FG. Inter-society consensus for the management of peripheral arterial disease (TASC II). *J Vasc Surg.* 2007;45(suppl S):S5–S67.
2. Fowkes FG, Rudan D, Rudan I, et al. Comparison of global estimates of prevalence and risk factors for peripheral artery disease in 2000 and 2010: a systematic review and analysis. *Lancet.* 2013;382:1329–1340.
3. Krishnamurthy P, Thal M, Verma S, et al. Interleukin-10 deficiency impairs bone marrow-derived endothelial progenitor cell survival and function in ischemic myocardium. *Circ Res.* 2011;109:1280–1289.
4. Rafii S, Lyden D. Therapeutic stem and progenitor cell transplantation for organ vascularization and regeneration. *Nat Med.* 2003;9:702–712.
5. Wu Y, Ip JE, Huang J, et al. Essential role of ICAM-1/CD18 in mediating EPC recruitment, angiogenesis, and repair to the infarcted myocardium. *Circ Res.* 2006;99:315–322.
6. Tateno K, Minamino T, Toko H, et al. Critical roles of muscle-secreted angiogenic factors in therapeutic neovascularization. *Circ Res.* 2006;98:1194–1202.
7. Chen L, Tredget EE, Wu PY, Wu Y. Paracrine factors of mesenchymal stem cells recruit macrophages and endothelial lineage cells and enhance wound healing. *PLoS One.* 2008;3:e1886.
8. Kebir A, Harhouri K, Guillet B, et al. CD146 short isoform increases the proangiogenic potential of endothelial progenitor cells in vitro and in vivo. *Circ Res.* 2010;107:66–75.
9. Tse HF, Siu CW, Zhu SG, et al. Paracrine effects of direct intramyocardial implantation of bone marrow derived cells to enhance neovascularization in chronic ischaemic myocardium. *Eur J Heart Fail.* 2007;9:747–753.
10. Grines CL, Watkins MW, Mahmarian JJ, et al. A randomized, double-blind, placebo-controlled trial of Ad5FGF-4 gene therapy and its effect on myocardial perfusion in patients with stable angina. *J Am Coll Cardiol.* 2003;42:1339–1347.
11. Kalka C, Masuda H, Takahashi T, et al. Vascular endothelial growth factor(165) gene transfer augments circulating endothelial progenitor cells in human subjects. *Circ Res.* 2000;86:1198–1202.
12. Takagi G, Miyamoto M, Tara S, et al. Controlled-release basic fibroblast growth factor for peripheral artery disease: comparison with autologous bone marrow-derived stem cell transfer. *Tissue Eng Part A.* 2011;17:2787–2794.
13. Wollert KC, Meyer GP, Lotz J, et al. Intracoronary autologous bone-marrow cell transfer after myocardial infarction: the BOOST randomised controlled clinical trial. *Lancet.* 2004;364:141–148.
14. Miyamoto M, Yasutake M, Takano H, et al. Therapeutic angiogenesis by autologous bone marrow cell implantation for refractory chronic peripheral arterial disease using assessment of neovascularization by ^{99m}Tc-tetrofosmin (TF) perfusion scintigraphy. *Cell Transplant.* 2004;13:429–437.
15. Tara S, Miyamoto M, Takagi G, et al. Prediction of limb salvage after therapeutic angiogenesis by autologous bone marrow cell implantation in patients with critical limb ischemia. *Ann Vasc Dis.* 2011;4:24–31.
16. Moriarty KT, Perkins AC, Robinson AM, Wastie ML, Tattersall RB. Investigating the capillary circulation of the foot with ^{99m}Tc-macroaggregated albumin: a prospective study in patients with diabetes and foot ulceration. *Diabet Med.* 1994;11:22–27.
17. Shida H, Oara I. Study on peripheral circulation using macroaggregated serum albumin labelled with radioactive iodine. *Angiology.* 1972;23:575–580.
18. Sturrock ND, Perkins AC, Wastie ML, Blackband KR, Moriarty KT. A reproducibility study of technetium-99m macroaggregated albumin foot perfusion imaging in patients with diabetes mellitus. *Diabet Med.* 1995;12:445–448.
19. Heck LL, Duley JW Jr. Statistical considerations in lung imaging with ^{99m}Tc albumin particles. *Radiology.* 1974;113:675–679.
20. Takagi G, Miyamoto M, Tara S, et al. Therapeutic vascular angiogenesis for intractable macroangiopathy-related digital ulcer in patients with systemic sclerosis: a pilot study. *Rheumatology (Oxford).* 2014;53:854–859.
21. Kelly JD, Forster AM, Higley B, et al. Technetium-99m-tetrofosmin as a new radiopharmaceutical for myocardial perfusion imaging. *J Nucl Med.* 1993;34:222–227.
22. Kawanaka H, Takagi G, Miyamoto M, et al. Therapeutic angiogenesis by controlled-release fibroblast growth factor in a patient with Churg-Strauss syndrome complicated by an intractable ischemic leg ulcer. *Am J Med Sci.* 2009;338:341–342.
23. Tara S, Takagi G, Miyamoto M, et al. Novel approach to ischemic skin ulcer in systemic lupus erythematosus: therapeutic angiogenesis by controlled-release basic fibroblast growth factor. *Geriatr Gerontol Int.* 2011;11:527–530.